Technical Report

UDC 621 . 771 . 073

Skin Pass Rolling Characteristics of Tin Plates with Dull Work Rolls —Numerical Analysis of Skin Pass Rolling of Tin Plates—

Tooru AKASHI* Toshiyuki SHIRAISHI
Shigeru OGAWA Yoshihito MATSUSE
Hideyuki MORIHARA

Abstract

A numerical analysis method for the skin pass rolling of tin plates with dull work rolls is established considering the surface asperity and elastic deformation of such work rolls. A rolling experiment using dull work rolls of comparable diameter to those used in commercial-scale skin pass rolling mills reveals higher elongation for smaller rolling force and much smaller elongation for larger rolling force compared with elongation behavior in the case of bright work rolls; such elongation characteristics also have predicted by the two-dimensional rolling FE analysis. Concerning surface roughness formation, it is found that the two-dimensional rolling FE analysis overestimates surface roughness compared with experimental results. To improve surface roughness prediction, a combination of two-dimensional rolling analysis with three-dimensional die press analysis simulating a generic piece of the rolled plate and a unit of asperity of the work roll is proposed.

1. Introduction

In skin pass rolling with dull work rolls of large diameter comparable to those used in commercial-scale skin pass rolling mills, it has been previously reported [1] that rolled plates exhibit minute elongation of less than 1% even when rolling force is so large that elongation of approximately 10% occurs in case of rolling with bright work rolls. No previous research based on numerical analysis concerning dull work roll rolling [2–4] has, however, succeeded to explain quantitatively this peculiar elongation behavior with dull work roll skin pass rolling.

Furthermore, in dull work roll rolling, realization of prescribed surface roughness of rolled plates are also important as well as giving prescribed elongation to rolled plates. Previously, a number of researchers have investigated on surface roughness transcription mechanism. Such investigations include: an experimental approach to show the surface roughness transcription characteristics by experimental rolling;[1] a quantitative approach using statistical parameters of the surface roughness obtained by electrical-discharge-machined dull work rolls and shot-blast-processed dull work rolls;[5] a simulation approach using a 3D die press analysis to simulate the 3D surface asperity confgulation;[6] an analysis of a 2D roll with asperity;[4, 7] a theoretical analysis using a slab method;[2] a study based on elastoplasticity FEM analysis;[8, 9] and so on. However, a comprehensively applicable method which is capable of explaining roll surface roughness transcription while incorporating the effect of roll diameter in a unified manner and predicting transcribed roughness has not yet been established.

In this report, based on the elastoplasticity rolling analysis method, which takes into account elastic deformation of work rolls appropriately, as shown in the explication of the rolling mechanism with bright work rolls of diameter comparable to those used in commercial scale rolling (previous report [10]), an analytical method that simulates the rolling phenomenon of elongation of less than 1% under lubricated rolling (friction) condition is developed by providing minute asperities on work rolls. The mechanism of dull work roll rolling and the rolling characteristics are examined using this analysis result, simultaneously proving the appropriateness of the analytical method.[11] Furthermore, by basing further study on numerical analysis of dull work roll rolling, focusing attention on the surface roughness transcription phenomenon on the rolled plate surface (transcribed by the roll surface asperities), and quantitatively comparing the results of experiment and numerical analysis concerning

* Chief Researcher, Dr.Eng., Integrated Process Research Lab., Process Research Laboratories
20-1 Shintomi, Futtsu City, Chiba Pref. 293-8511

the roughness of *Ra*, the mechanism of surface roughness transcription is clarified, and a comprehensive method of predicting transcribed roughness is proposed.[12)]

2. Experiment of Dull Work Roll Rolling and Numerical Analysis

2.1 Experimental skin pass rolling

In the experiment, a tin plate sheet of 0.2 mm in thickness and 150 mm in width, the same size as the one used in the previous report,[10)] was used, and the elongation was measured by measuring the distance between two scratched lines. The standard rolling condition is shown in **Table 1**. The experiment was conducted under the same conditions of emulsion lubrication as in the experiment in the previous report, and also without lubrication.

2.2 Result of experiment

Figure 1 shows the result of the experiment with dull work roll rolling and, for comparison, the result of an experiment with bright work roll rolling using rolls of ϕ480 mm in diameter and the result of a simulation. In the case of bright work rolls, the occurrence of a jumping phenomenon of a sharp rise in elongation in the vicinity of 2.5 MN · mm^{-1} of rolling force per unit width is observed. In dull work rolls, however, elongation of less than 1% is observed. Next, referring to **Fig. 2**, where the elongation scale of Fig. 1 is magnified, in the rolling force region just before the start of the jumping, it is found that the elongation in case of dull work roll rolling is larger than that in the case of bright work roll rolling. It is the characteristics of dull work roll rolling that the elongation starts to rise at a rolling force as low as 0.5 MN · m^{-1} and reaches 0.4% before reaching 2.5 MN · m^{-1}, where the jumping in bright roll rolling starts. This is then followed by elongation increases at a moderate rate.

2.3 Elastoplasticity FEM model for skin pass rolling

Elastoplasticity FEM analysis general software (MSC.Marc) is used to obtain numerical solutions. The object of numerical analysis is a 2D model based on plane strain elements as shown in **Fig. 3**, and it is assumed that the work roll is an elastic body and the rolled plate is an elastoplastic body having upper and lower yield points. Although the asperity on the roll surface is 3D in nature, the analysis was conducted under the assumption of a 2D plane strain condition. Although asperity is 3D in nature, it is considered that the assumption of 2D plane strain condition is reasonable in macroscopic context as asperity constrains the strain in the widthwise direction when it penetrates into a plate.

In order to provide the fan-shaped roll with the same rigidity of the entire solid roll, a rigid beam which only allows the displacement in radial direction is provided on either side of the fan. The analysis was conducted under a condition where the work roll is turned by forced displacement and the rolling force is added gradually as is in the case of the experiment, and relation between the elongation of the rolled plate and rolling force was observed.

Further, although the mathematical average of the roll surface roughness *Ra* used in the experiment is $Ra \fallingdotseq 3.1–3.3\mu$m, the roll surface asperity configuration was modelled considering that the peak value of the actual asperity is larger than *Ra*. To be specific, since the average of asperity is 0.637*D* (as shown in Formula (1)) when the configuration of asperity is represented by a sine wave curve and its half amplitude is expressed as *D*, in the FEM analysis, the asperity configuration was assumed to be represented by a triangular-shaped wave of which the maximum half amplitude was set as $D = 3.2\mu\text{m}/0.637 \fallingdotseq 5\mu$m (10 μm for whole amplitude). In **Fig. 4**, the relationship between the sine wave curve corresponding to

Table 1 Rolling conditions

Work roll (WR)	ϕ480 mm × 400 mm width Roughness: 3.1–3.3 μmRa (shot dull)
Lubrication	5% emulsion (50°C), no lubrication
Tin plate	Thickness: 0.2 mm, Width: 150 mm Upper yield stress: 400 MPa Lower yield stress: 312 MPa
Rolling condition	Entry unit tension: 82 MPa Delivery unit tension: 98 MPa Rolling speed: 10 m/min

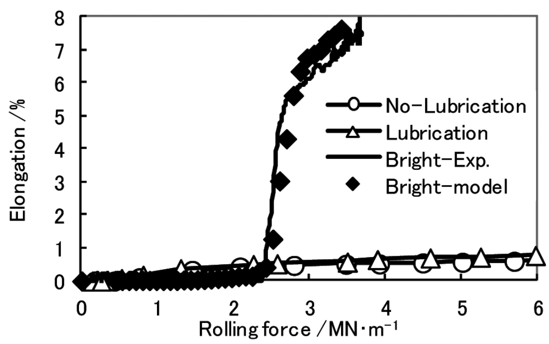

Fig. 1 Elongation of rolled tin plate with dull and bright rolls

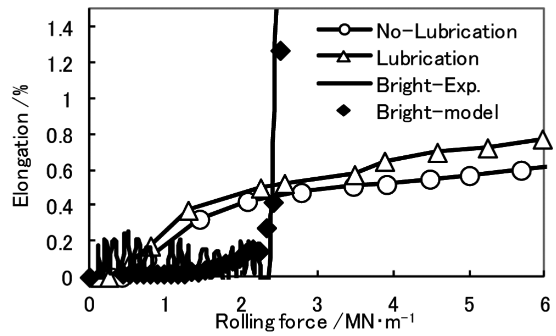

Fig. 2 Elongation of rolled tin plate with dull and bright rolls (enlargement)

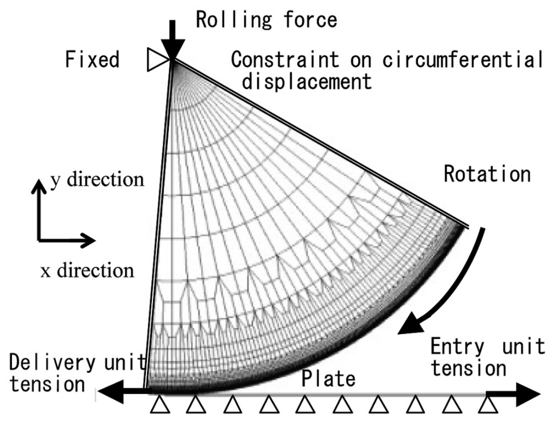

Fig. 3 FEM model of skin pass rolling

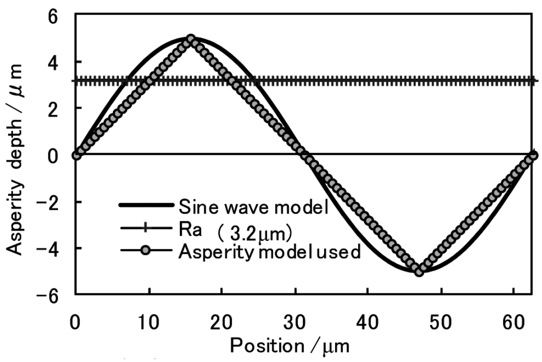

Fig. 4 Roll surface asperity model

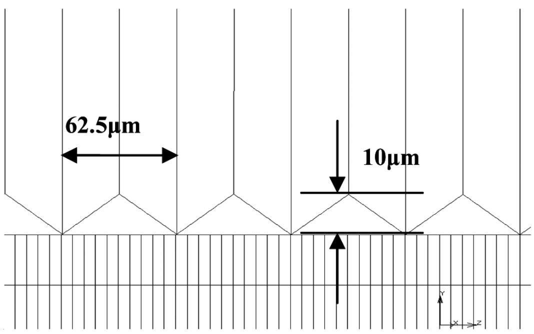

Fig. 5 Magnified finite element mesh at roll-plate interface

$Ra = 3.2\,\mu$m and the triangular-shaped wave used in the FEM analysis is shown. Magnified figures, illustrating the roll surface asperity configuration and the rolled plate fine element mesh, are shown in **Fig. 5**.

$$dave = \frac{1}{\ell}\int_0^{\ell} \left| D \cdot \sin\left(2\pi x/\ell\right) \right| dx = \frac{2D}{\pi} = 0.637D \qquad (1)$$

where ℓ : wave length of a sine curve (μm)
x : displacement (μm)
D: half amplitude (μm)

Since the object of the calculation is the experiment conducted under lubricated conditions and using the rolled plate, both being the same as those in the experiment conducted in the previous report on bright work roll rolling,[10] to meet the conditions of Table 1 to maintain conformity of the rolling analysis to bright work roll rolling, a shear friction model is used to model friction. The values of the friction factor m (friction stress/shearing yielding stress) are the same as those used in the previous report,[10] i.e., $m = 0.2$ with lubrication and $m = 0.275$ without lubrication. As annealed tin steel material plate was used as the rolled plate, and the flow stress was set as shown in **Fig. 6**. An FEM model was developed, and the analysis was conducted based on the above-mentioned prerequisites pertaining to roll surface and lubrication as summarized in **Table 2** and under the rolling conditions prescribed in Table 1.

2.4 Comparison of results of numerical analysis and experiment

Figures 7 and **8** show the state of contact of a roll with a rolled plate being rolled under the rolling force of $2\,\mathrm{MN \cdot m^{-1}}$, and a magnified version of the same figure, respectively. These are shown as examples of states of rolling obtained with numerical analysis. In both figures, the scale in the thickness direction is magnified by 29 times the scale in the rolling direction. From Figs. 7 and 8, it is found that in dull work roll rolling, the work roll itself is flattened in a nearly symmetrical manner in the rolling direction, plastic deformation starts at the roll surface asperity, and the plastic deformation develops mainly in the surface part of the rolled plate.

Next, as shown in **Figs. 9** and **10**, is change in elongation strain in the rolling direction averaged in the thickness direction when the

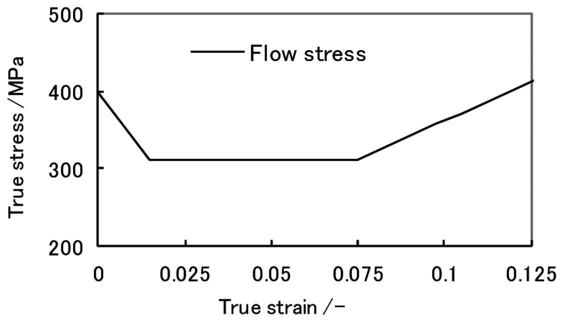

Fig. 6 Flow stress used in the analysis

Table 2 Roll surface and lubrication conditions

WR asperity	Roughness: 3.1–3.3 μmRa (shot dull) → Triangle wave type Asperity height: 10 μm Asperity pitch: 62.5 μm
Lubrication	5% emulsion (50 °C) → $m = 0.2$ No lubricating → $m = 0.275$

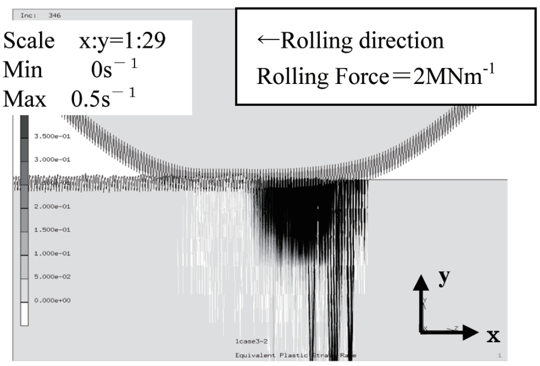

Fig. 7 Rolling configuration and equivalent plastic strain rate

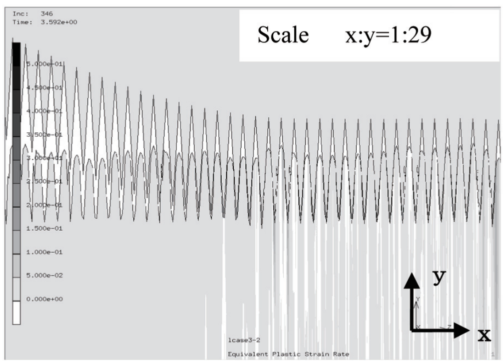

Fig. 8 Rolling configuration and equivalent plastic strain rate (enlargement)

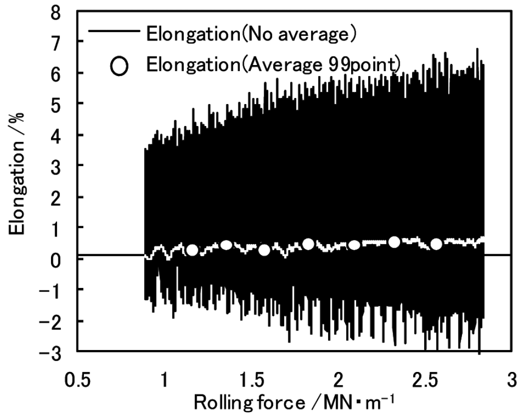

Fig. 9 Relation between elongation and rolling force

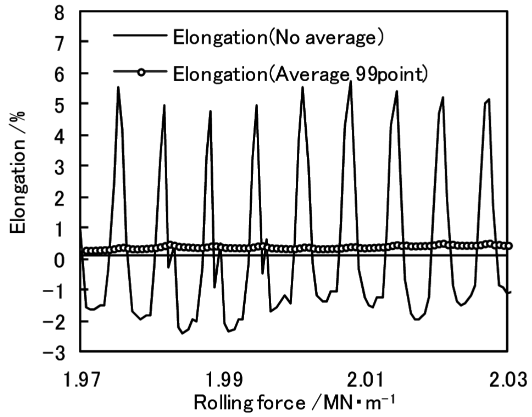

Fig. 10 Relation between elongation and rolling force (enlargement)

rolling force is gradually increased. Since the elongation strain fluctuates greatly in the rolling direction during a cycle of roll surface asperity, the data was smoothed by applying a moving average method. Further, it is considered that the aforementioned fluctuation of elongation strain is attributed to influence exerted by the asperity of the roll surface. The height of asperity of 10 μm employed in this research corresponds to 10% of the half thickness (0.1 mm) of the plate (plate thickness 0.2 mm) and, therefore, is a significantly large figure for rolling elongation of less than 1%. As a result, the reduction in thickness and elongation fluctuate cyclically and noticeably, and absolute value of the fluctuation becomes approximately five times the average of the elongation strain. In this article, the moving-average of the elongation strain is, hereinafter, used as the value of elongation.

In **Fig. 11**, the relationship between rolling force and elongation calculated corresponding to the experiments shown in Figs. 1 and 2 is shown. The calculated elongation shows excellent agreement with the experimental results, with the friction factor finely adjusted to $m=0.2$ for the lubricated case and $m=0.275$ for the case without lubrication.

In addition, the results of experiments and calculations with respect to the jumping phenomenon that appeared in the rolling with bright work rolls as described in the previous report[10] are also shown in Fig. 11. The figure shows that, in this analysis, relationships between the rolling force and elongation under both conditions of bright work roll rolling and dull work roll rolling are both in good agreement with the experimental results by just modeling roll surface configurations (bright or dull) adequately withoutchanging the friction factor. This indicates appropriateness and versatility of the analysis.

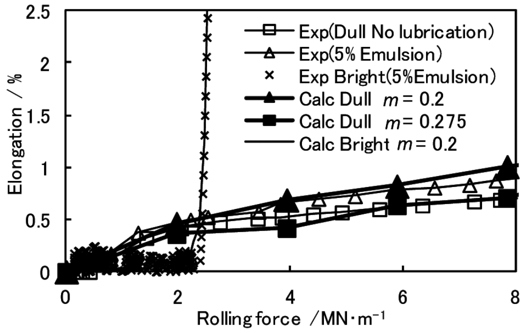

Fig. 11 Comparison of calculation with experiment on elongation of rolled plate with dull rolls

3. Examination of Rolling Phenomenon with Dull Work Rolls Based on Numerical Analysis

As described in the previous chapter, by using the analysis method, which accurately takes into account the elastic deformation of a work roll and the elastoplastic deformation of a rolled plate, accurate numerical analysis of rolling with large diameter dull work rolls, which had been impossible in previous research, has become possible. In this chapter, sensitivity analysis is conducted on influences of friction factor and roll surface asperity on relationship between rolling force and elongation by using this analysis method, and rolling phenomena with dull work rolls are further examined.

3.1 Influence of friction factor

In order to examine influences of roll surface asperity and friction factor on elongation, according to the results of calculations, relation between elongation and rolling force per unit width is shown with friction factor *m* as a parameter in **Fig. 12**. As for any friction factor, the elongation increases as the rolling force increases. Further, the elongation increases as the friction factor becomes smaller. However, it is clarified that the rolling is stably conducted without slipping at the whole contact arc length even when the friction factor is set to be zero ($m=0$) as an ultimate friction condition. This is considered to be attributed to the geometrical frictional effect caused by the plastic deformation of the rolled plate developed by the roll surface asperity. Specifically, at the very moment asperity locally contacts the rolled plate, the plastic deformation is developed immediately at the point of contact by stress concentration, and, with the asperity penetrating deeply into the rolled plate by 5% of the entering plate thickness, the slope of the roll surface asperity and the rolled plate form a substantial contact area. It is considered that the component in the rolling direction of the force working perpendicular to the slope acts as an apparent frictional force upon the rolled plate.

Further, relationship between elongation and the stress in the rolling direction averaged in the entire roll bite region (which is arranged with respect to the friction factor) is shown in **Fig. 13**. From Fig. 13, it is found that for the same elongation, the higher the friction factor is, the higher the compressive stress in the rolling direction becomes. It is reasoned that, in addition to the aforementioned geometrical friction force, as the friction factor becomes higher, the friction force acting on the slope of the roll asperity and the rolled

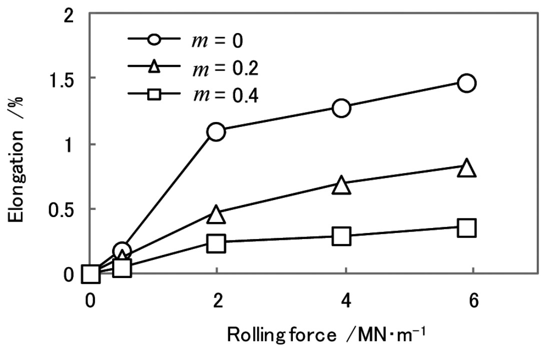

Fig. 12 Effect of friction factor on elongation

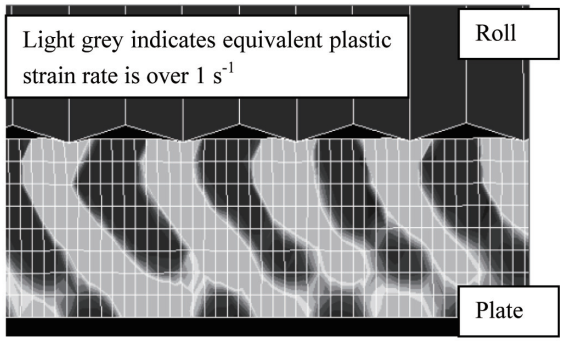

Fig. 14 Equivalent plastic strain rate at roll bite ($m=0$)

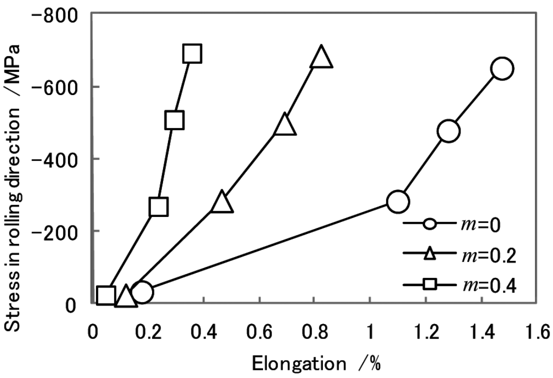

Fig. 13 Relation between elongation and stress in rolling direction

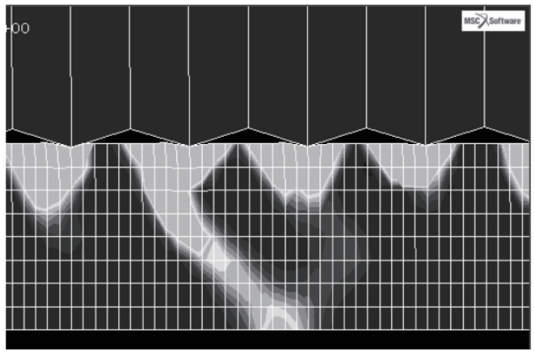

Fig. 15 Equivalent plastic strain rate at roll bite ($m=0.4$)

plate becomes higher, and its component in the rolling direction is added to the apparent friction force. Therefore, the compressive stress in the rolling direction acting in the rolled plate increases. As the compressive stress in the rolling direction increases, the rolling force increases according to the yield condition, and the rolling force increases for a given elongation, as shown in Fig. 12.

Next, the aforementioned phenomenon is examined under an identical rolling force condition. **Figures 14** and **15** show distributions of plastic strain rate at the identical rolling position in the vicinity of the entry of the roll-bite in the case of a rolling force of $4\,MN\cdot m^{-1}$ and friction factors m of 0 ($m=0$) and 0.4 ($m=0.4$). The light grey area on the rolled plate shows the domain where the high equivalent plastic strain rate of higher than $1\,s^{-1}$ is taking place. However, a big difference is noticed when the rolling states in Figs. 14 and 15 are compared.

In the case of Fig. 14, where the friction factor $m=0$, the plastic deformation domain starting at the roll asperity penetrates through the entire plate thickness, thereby contributing to the elongation of the rolled plate. However, contrarily to the above, in the case shown in Fig. 15, where $m=0.4$, most of the plasticity domain starting at the roll asperity stays in the vicinity of the surface, does not contribute to elongation, and forms a pattern of plasticity domain similar to that which takes place when pressing a punch into a bulk body with sufficient thickness. This is caused because when the friction factor is high, the compressive stress in the rolling direction becomes higher, and the deviatoric stress components, the source of plastic strain in rolling direction, become smaller.

3.2 Effect of height of roll surface asperity

As examined in the above section, the roll surface asperity is the most crucial factor that characterizes the dull work roll rolling.

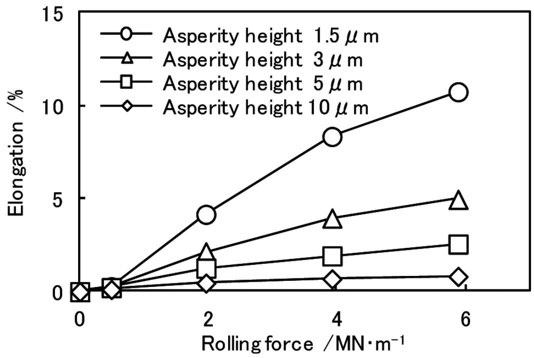

Fig. 16 Effect of roll asperity height on elongation

Thereafter, the effect of the configuration of the roll surface asperity on the rolling characteristics is examined. Firstly, the friction factor m is assumed to be 0.2, and the height of the asperity is varied from 1.5 to 10 μm without changing the pitch of the asperity. Relationship between rolling force and elongation is shown in **Fig. 16**. From Fig. 16, it is found that the higher the asperity height becomes, the smaller the elongation becomes and vice versa. This is explained as follows; as the asperity becomes sharp as the height of the roll surface asperity becomes larger, and as the asperity penetrates deep into the rolled plate, the area of contact increases. Moreover the gradient of the asperity slope becomes larger, and therefore rolling direction component of the contact pressure acting between the roll and the rolled plate increases, and the apparent friction force is thus increased.

3.3 Effect of roll surface asperity pitch

Next, the effect of the roll surface asperity pitch is examined.

Figure 17 shows the relationship between the rolling force and elongation when the pitch of the asperity is changed from 62.5 to 187.5 μm while the friction factor is assumed as 0.2 (m=0.2) and the height of the asperity (10 μm) is unchanged. From Fig. 17, it is found that the smaller the asperity pitch becomes, the smaller the elongation becomes. This phenomenon is attributable to the mechanism similar to the one in the case of the effect of asperity height. Specifically, as the asperity pitch becomes smaller, the roll surface asperity becomes sharp, the number of asperity pitches per unit area increases, and, therefore, the contact area between the roll and plate increases relatively. In addition, the gradient of the asperity slope becomes larger, and thereby the component in the rolling direction of the contact pressure between the roll and the rolled plate becomes higher and the apparent frictional force is increased.

3.4 Effect of the angle of slope of roll surface asperity

So far the effect of roll surface asperity has been examined from the viewpoints of height h and pitch p. The angle of slope of the roll surface asperity was also examined as it is also considered to be a crucial factor. The gradient of the roll surface asperity defined by the asperity pitch p and height h in the formula (2) was sought for, and its effect on the elongation under the condition of 4 MN · m^{-1} was arranged, the result of which is shown in **Fig. 18**.

$$grad = \frac{h}{(p/2)} \qquad (2)$$

From Fig. 18, as examined so far, it is confirmed that as the asperity slope angle becomes higher, the elongation decreases. Further, in Fig. 18, the results of the cases where asperity height and pitch are changed are plotted. In both cases, the plotted results stay on an almost hyperbolic curve. This is considered to indicate that the angle of roll surface asperity is a dominant factor over the apparent frictional force in dull work roll rolling.

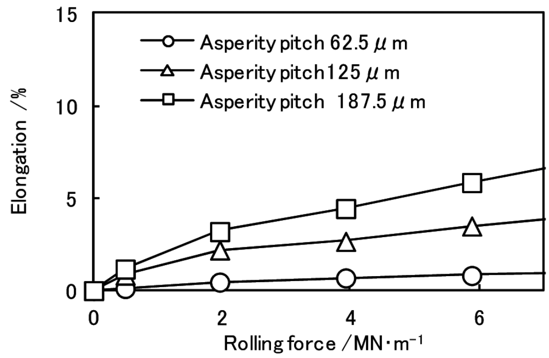

Fig. 17 Effect of roll asperity pitch on elongation

3.5 Relationship between roll displacement and rolling force and elongation

Next, in order to examine relationship between roll deformation and rolled plate deformation in a quantitative manner, an examination is conducted focusing on roll displacement in the direction of reduction, namely, a parameter equivalent to reduction control input. Shown in **Fig. 19** is relationship between displacement of a roll in the direction of reduction, or the amount of reduction, and rolling force calculated for three levels of friction factor shown in Figs. 12 and 13.

From Fig. 19, it is found that an approximately proportional relationship exists between the amount of reduction and the rolling force, regardless of the friction factor. When skin pass rolling is imaged based on this result together with the result in Fig. 12, the rolling force is determined almost unambiguously when the amount of roll reduction is given. However, Fig. 12 shows that the elongation obtained at the time varies greatly depending on the friction factor. This situation seems to be different from the teachings of the classical theory of rolling that rolling force and then delivery plate thickness are determined by entry thickness and roll gap i.e. roll reduction position. In the classical theory of rolling, when the roll reduction position is given, the rolling force and elongation correspond to each other on a one-to-one basis. However, Figs. 12 and 19 show that the rolling force and elongation, namely, plate thickness, do not correspond to each other on a one-to-one basis.

The aforementioned phenomenon of dull work roll rolling is understood as follows. From Fig. 12, it is found that the elongation of the rolled plate obtained in the rolling force region in the current study is approximately 1%, which is equivalent to approximately 2 μm of reduction in plate thickness for entry plate thickness of 0.2 mm. On the other hand, the amount of roll reduction observed in Fig. 19 is about 50 μm on one side and becomes about 100 μm with upper and lower side rolls together. Accordingly, it is understood that most of the roll reduction change is absorbed by roll flattening deformation without causing noticeable change in plate thickness. Specifically, in the rolling condition where elongation of about 1% for a thin steel plate of 0.2 mm in thickness, reduction change in plate thickness that renders elongation change is negligibly small as compared to change in roll flattening deformation, and change in the apparent plasticity coefficient of the rolled plate varies greatly depending on the difference in the frictional condition. With these two factors taken into account, an understanding of the rolling phenomenon in dull work roll rolling based on the extended viewpoint of classical theory of rolling becomes possible.

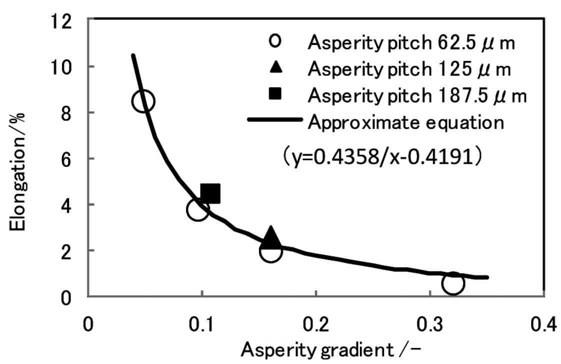

Fig. 18 Effect of roll asperity angle on elongation

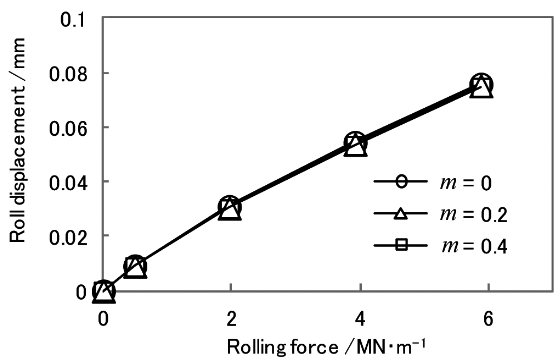

Fig. 19 Relation between roll displacement and rolling force

4. Examination of Difference from Bright Work Roll Rolling

4.1 Difference of plastic deformation characteristics in low rolling force region

Concerning the phenomenon in the high rolling force region that elongation in dull work roll rolling becomes smaller compared to elongation in bright work roll rolling, the study made so far has clarified that the phenomenon can be explained by taking into account the geometrical friction effect exerted by the dull work roll surface asperity. In this section, the low rolling force region, where elongation in dull work roll rolling becomes higher than the elongation in bright work roll rolling, is examined.

The average values of equivalent plastic strain rate and equivalent strain in the thickness direction, within the arc of contact in the case of the friction factor $m=0.2$ and a rolling force of $2\,MN\cdot m^{-1}$, are shown in **Figs. 20** and **21**, respectively. In Figs. 20 and 21, rolling phenomena of dull work roll rolling and bright work roll rolling are compared under an identical rolling force from the viewpoint of plastic strain. As the examination in the foregoing chapter shows, the amounts of roll flattening of bright and dull work rolls are nearly the same. However, in the case of dull work roll, the apparent length of contact arc shown in Figs. 14 and 15 is increased by the roll surface asperity, and large plastic deformation is produced by penetration of the roll surface asperity into the rolled plate.

Under the rolling force of $2\,MN\cdot m^{-1}$, in bright work roll rolling, jumping has not yet occurred as shown in Fig. 11, and although the generation of a slight equivalent plastic strain rate and an equivalent plastic strain of about 0.002 are observed in Figs. 20 and 21, respectively, in the flow stress model shown in Fig. 6, the flow stress stays in the neighborhood of the upper yielding point. On the other hand, in dull work roll rolling, as shown in Figs. 14 and 15, an equivalent plastic strain rate higher than $1.0\,s^{-1}$ is generated, starting at the asperity, and as confirmed in Fig. 20, the equivalent plastic strain exceeds 0.015 near the entry of roll bite, at which value the lower yielding point is reached. Specifically, it can be explained that in the dull work roll rolling condition, flow stress of the rolled plate reaches the lower yielding point at the earlier stage with the penetration of the roll surface asperity into the rolled plate, and an elongation higher than the one just before the start of jumping in the bright work roll rolling condition is observed.

4.2 Examination concerning rolling tension

In the previous report,[10] it was clarified that in the bright work roll rolling condition where jumping had already started, the exit side tension has a greater influence on elongation than the entry side tension. In this work, the initial entry and exit side tensions were set to 82 and 98 MPa for dull work roll rolling, and then the change in elongation vs rolling force was recorded as the entry and exit side tensions were varied.

The results are shown in **Figs. 22** and **23**. It was found that in the case of dull work roll rolling, unlike in bright work roll rolling, the entry side tension has a greater influence on elongation than the exit side tension. It is presumed that, as examined in Fig. 20, in bright work roll rolling after jumping, plastic strain is concentrated on the

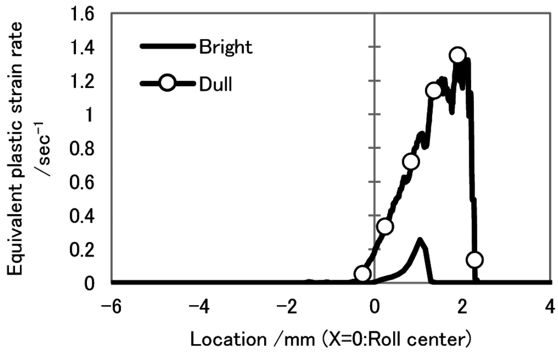

Fig. 20 Distribution of equivalent plastic strain rate along the roll-bite ($m=0.2$)

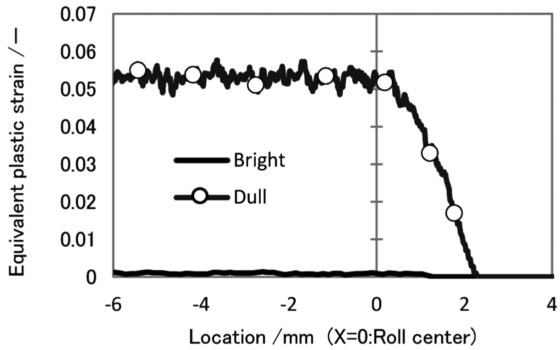

Fig. 21 Variation of plastic strain in the rolling direction along the roll-bite ($m=0.2$)

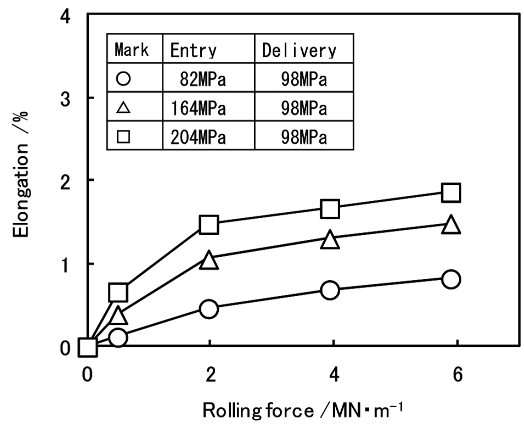

Fig. 22 Effect of entry tension on elongation

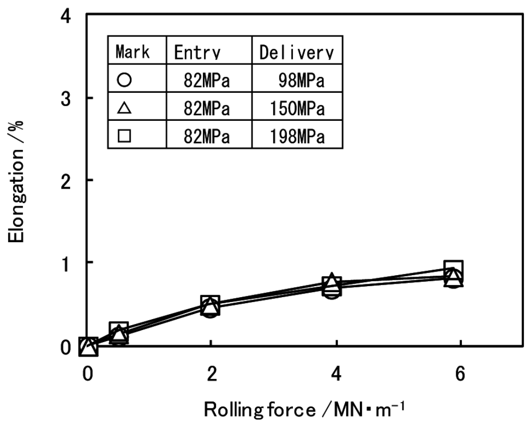

Fig. 23 Effect of delivery tension on elongation

latter half of the contact arc length. However, in dull work roll rolling, the plastic strain rate takes place on the entire contact arc length. Furthermore, since the remarkable plastic strain rate takes place at the entry of the roll bite, the influence of entry side tension becomes higher.

5. Transcription of Asperity Studied with Dull Work Roll Rolling Analysis

Next, mechanism of asperity transcription phenomenon is examined. **Figure 24** shows an example of roll surface asperity and transcribed asperity configurations on the steel plate right after the exit from the roll bite after the completion of rolling in the aforementioned dull work roll rolling analysis. Based on the aforementioned result of the analysis of skin pass dull work roll rolling and focusing on the transcribing phenomenon of roll surface asperity which results in the transcribed configuration on the steel plate surface, the calculated and experimental values obtained for surface roughness, *Ra*, are compared.

5.1 Outlines of experiment and numerical analysis model

The calculation and experiment conditions, including the surface asperity specification, are the same as those used in the aforementioned approach except the size of the roll diameter. **Table 3** shows analysis and experimental conditions.

5.2 Effect of roll diameter on rolling force and elongation

With respect to relationship between rolling force and elongation, results of experiment and analysis are compared and shown in **Fig. 25**. Both with a large diameter roll of ϕ480 mm and a newly added small diameter roll of ϕ165 mm, the results showed good agreement under the lubricating condition of $m=0.2$. Although, under the condition of no lubrication, the experimental result has an elongation value around 10% less with respect to the calculated rolling force, it is judged that this numerical analysis represents sufficiently and appropriately the relationship between rolling force and elongation in dull work roll rolling, including a clear distinction in the difference in roll diameter sizes and lubricating effects.

In **Fig. 26**, the magnified minute rolling force region is shown together with the result of the case of a small diameter roll in bright work roll rolling reported in the previous paper.[10] In bright work roll rolling, as compared to the dull work roll rolling condition, in the rolling force region of above 0.5 $NM \cdot m^{-1}$, the elongation sharply increases with respect to rolling force. Then, in order to clarify the characteristics of rolling with the respective rolling condition, configurations of the roll and the plate and the equivalent plastic strain rate distribution in the vicinity of the roll bite are shown in **Fig. 27**.

From this result, in the bright work roll rolling of ϕ165 mm, where roll surface asperity is not provided, although slight roll flattening is observed, the arc of contact is close to a perfect circle in shape, and therefore the state of rolling is considered to be the same as that of the general classical theory of rolling where plastic deformation progresses along the entire region of roll bite, from the roll bite entry to the delivery. On the other hand, the large diameter dull work roll is flattened on the entire region of contact with the plate and looks as if it contacts with the plate in a parallel manner. Likewise, in the dull work roll rolling with ϕ165 mm, roll flattening exists. However, as compared to the case of a large diameter roll, the plastic strain rate in the neighborhood of the roll bite entry is large and reaches the plate thickness center. It is considered that, as com-

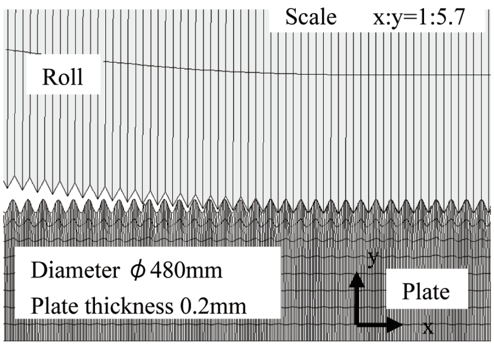

Fig. 24 Transcription of the roll surface asperity (in delivery side)

Table 3 Rolling conditions

WR	(ϕ480 mm, ϕ165 mm) × 400 mm width, Roughness: 3.1 - 3.3 μmRa (shot dull) → Asperity height: 10 μm Asperity pitch: 62.5 μm
Lubrication	5% emulsion (50°C) → $m=0.2$ No lubricating → $m=0.275$
Plate	Thickness: 0.2 mm, Width: 150 mm Upper yield stress: 400 MPa Lower yield stress: 312 MPa
Rolling conditions	Entry unit tension: 82 MPa Delivery unit tension: 98 MPa Rolling speed: 10 m/min

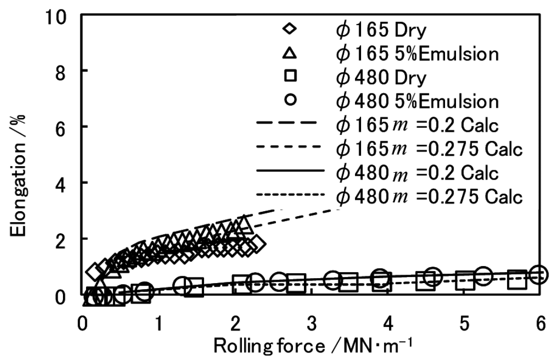

Fig. 25 Elongation of rolled plate with dull rolls

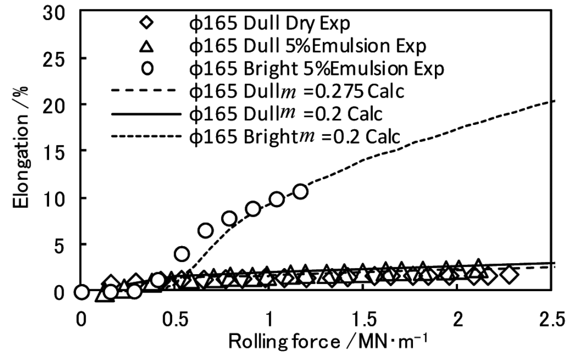

Fig. 26 Elongation of rolled plate with dull and bright rolls

pared to the case of large diameter work roll rolling, the roll and the plate contacts at a more acute angle geometrically, and as a result, stress concentration and significant plastic deformation take place. However, even in the small diameter roll case, hydrostatic stress becomes higher, and elongation becomes smaller compared to the case of bright work roll rolling due to the geometrical friction effect of surface asperity.

From the above, the numerical analysis is judged to be a calculation method of high universality because the calculated result which has high conformity to the experimental result as to the relationship between rolling force and elongation has been obtained in each skin pass rolling condition, including with small and large diameter rolls.

5.3 Transcription form of roll surface asperity

The form of transcription of the roll surface asperity to the plate is explained based on the numerical analysis.

Figure 28 is the magnified figure showing the state of contact of asperity in the neighborhood of entry to the roll bite and stress distribution in the rolling direction (x) under the condition of a ϕ 165 mm roll, a rolling force of 2 MN · m^{-1}, and an elongation of 2.3%. It is found that the front tension of 82 MPa uniformly developed in the thickness direction (y) at the roll bite entry transforms to compressive stress toward the thickness center from the surface as rolling progresses toward the roll bite center, and asperity penetrates into the plate corresponding to the increase in compressive stress. The space of the asperity is filled in with the plate material.

Furthermore, for the purpose of observing the geometrical change in the neighborhood of roll bite in a quantitative manner, the displacement of the utmost surface of the steel plate and the moving average values are shown in **Fig. 29**. It is found that at the moment the roll surface asperity starts to contact, the average plate thickness starts to decrease and starts to elongate, and the roll surface asperity is transcribed. Transcription progresses even after the gradient of reduction in the plate thickness becomes gentle, the plate material gradually fills in the asperity space, and finally the position of the apex of the asperity on the plate becomes about 2 μm above the original plate thickness.

At this point, the relationship between the stress in the rolling direction in the roll bite and its neighborhood is averaged in the plate thickness direction, and the height of the surface asperity transcribed on the plate plotted in the rolling direction is shown in **Fig. 30**. Transitions in the roll bite of stress $\overline{\sigma}_x$ in the rolling direction (x) and the stress σ_y in plate thickness direction (y) are shown in **Fig. 31**.

Further, since one cycle of surface asperity height has 12 nodes, the maximum and minimum values of surface nodes in the section of the front and rear 6 nodes in the rolling direction were sought for, and the difference was defined as the asperity height. Furthermore, as for the stress in the plate thickness direction, the value of the outermost surface was used. However, as a large stress fluctuation corresponding to the asperity cycle is caused and affects the surface asperity if the value is used unprocessed, moving average processing was applied by using the values of the front and rear sections of a node. In the calculation result shown in Fig. 30, from the roll bite entry toward the center, as the compressive stress in the rolling direction becomes higher, the surface asperity height grows higher, and the asperity transcription saturates in the neighborhood of the roll bite center where compressive stress in the rolling direction reaches a peak. Furthermore, as observed in Fig. 31, stress in the

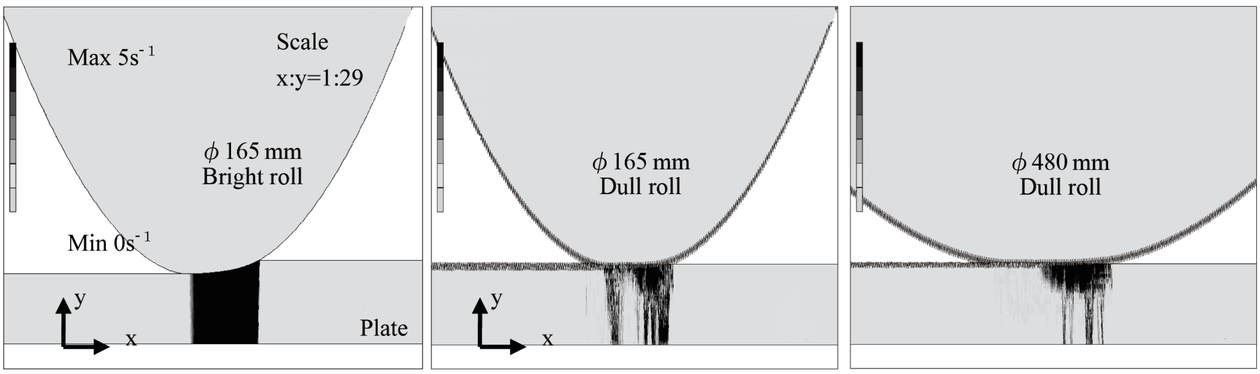

Fig. 27 Distribution of plastic strain rate around the roll bite with ϕ 165, 480 mm dull and ϕ 165 mm bright rolls at rolling force 2 MN·m^{-1}

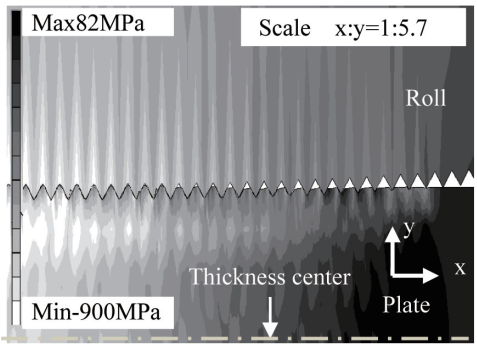

Fig. 28 Stress in rolling direction at rolling force 2 MN·m^{-1}

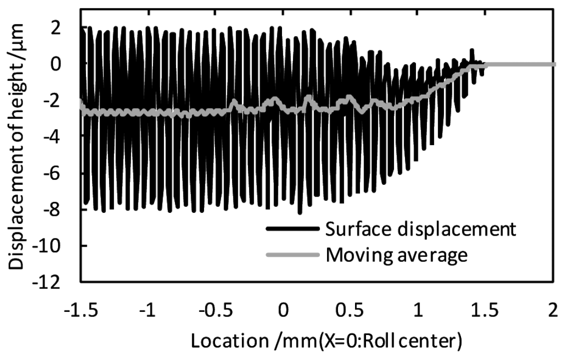

Fig. 29 Geometrical changes around the roll bite (with ϕ 165 mm roll)

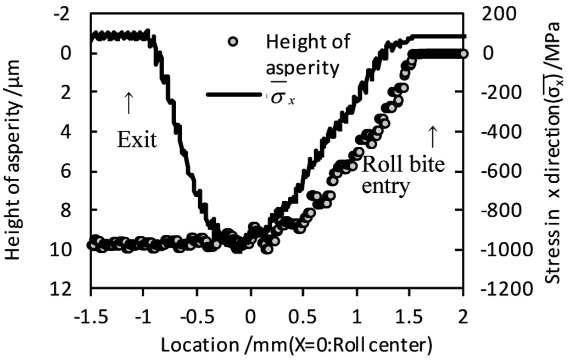

Fig. 30 Relation between asperity height and stress in rolling direction (ϕ165mm, rolling force 2MN·m^{-1})

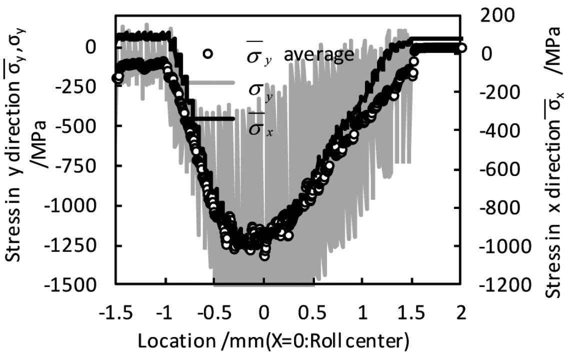

Fig. 31 Relation between stress in rolling direction and stress in thickness direction (ϕ165mm, rolling force 2MN·m^{-1})

plate thickness direction has a strong correlation with stress in the rolling direction, and transcription of asperity is generated as the hydrostatic pressure increases. From these results, it is understood that the transcription phenomenon of asperity is closely correlated to stress in the rolling direction, stress in the thickness direction, and hydrostatic pressure within the roll bite.

5.4 Assessment of roughness transcription analysis

Shown in **Figs. 32** and **33**, respectively, are the results of experiment and numerical analysis conducted for the surface roughness *Ra* of the rolled plate after dull work roll rolling plotted vs rolling force for a 165 and a 480 mm diameter roll. In the calculation for the small diameter roll (165mm diameter), the transcribed roughness *Ra* is not dependent on changes in the friction factor. However, in the experiment result, the surface roughness in case of no lubrication is slightly larger under an identical rolling force. However, as long as there is no lubrication, the experimental and calculated results show good agreement with each other. On the other hand, in the experiment with a large diameter roll of ϕ480mm, transcription progresses more slowly than in the case of a small diameter roll, even under a higher rolling force. Above a rolling force of 4MN·m^{-1}, the surface roughness *Ra* transcribed under no lubricating condition becomes slightly larger. For this, the calculated results predict *Ra* larger by 20–30% than that obtained experimentally, and, as in the case of small diameter rolls, the effect of friction factor is not noticed.

Next, in **Figs. 34** and **35**, the relationship between the transcribed roughness *Ra* and elongation are shown for comparison. As for the small diameter roll of ϕ165mm, in the arrangement as to

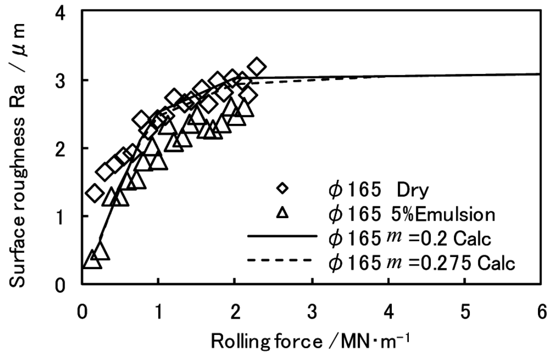

Fig. 32 Relation between surface roughness and rolling force (with ϕ165mm roll)

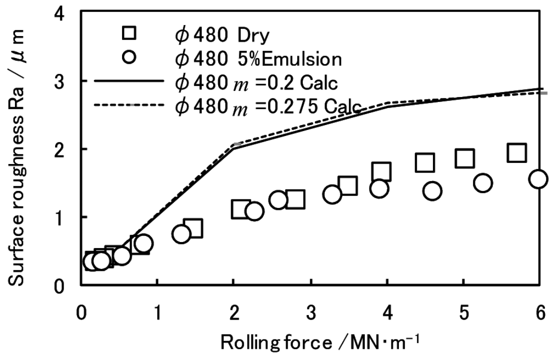

Fig. 33 Relation between surface roughness and rolling force (with ϕ480mm roll)

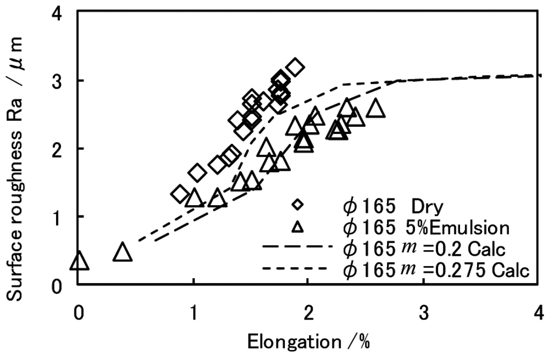

Fig. 34 Relation between surface roughness and elongation (with ϕ165mm roll)

the rolling force in Fig. 32, the effect of the friction factor *m* is not noticed, but the difference appears when the surface roughness *Ra* is examined from the viewpoint of elongation. However, in the case of a large diameter roll of ϕ480mm, although the effect of friction factor emerges, the results do not agree quantitatively.

As the resistance of oil contained between the roll and plate is not taken into account in this approach, it is considered that certain limit can't be helped in the discussion of transcription mechanism in lubricated condition. According to the literature, there is a case [13] wherein transcription of surface roughness *Ra* is suppressed to a smaller scale by incompressible oil caught in between the roll surface and plate in rolling with lubrication. Therefore, in the following section, an examination will be made limiting to the case of transcription under no lubrication condition.

6. Examination of Roughness Transcription Phenomenon

6.1 Examination of asperity transcription phenomenon with 3D die press analysis

Up to now, the transcription characteristics of surface asperity have been shown with 2D rolling analysis based on a plain strain condition. In the case of the small diameter roll, the predicted roughness *Ra* agreed with the actually measured values in an approximately quantitative manner. However, in the case of the large diameter roll, an error reaching 20–30% was generated. As the cause of the error, it was presumed that the 3D asperity of actual rolls having its convexo-concave configuration in the width direction is the cause of the error. Then, the transcription phenomenon and its mechanism were examined by conducting a simplified 3D die press numerical analysis, wherein a die tool element of minimum unit of one cycle of roll surface asperity is assumed, and the boundary conditions are established in such a way that $\bar{\sigma}_x$ and elongation agree with the results obtained with the 2D rolling analysis. $\bar{\sigma}_x$ is the stress in the rolling direction averaged in the plate thickness direction and considered to be the major factor in transcription.

(1) Analysis model

The model was a rectangular parallelepiped of 0.1 mm × 0.0625 mm × 0.0625 mm in size, with a plain strain condition in the width direction. When 2D rolling was simulated, the die tool was modeled as a triangular prism having its generating line in the width direction (hereinafter referred to as 2D asperity), and when 3D rolling corresponding to an experiment was simulated, the die tool was modeled as a square pyramid (hereinafter referred to as 3D asperity). Furthermore, the hatched square pyramid of the 3D die tool shown in **Fig. 36** is upwardly convex, and the other is downwardly convex. The height of the 2D asperity was defined as the distance between the top and bottom peak of the asperity as originally defined and was set at 10 μm. The height of the 3D asperity was set at 15 μm (half amplitude 7.5 μm) so that the mathematical average of roughness becomes equal (the averages of the absolute heights of roughness of die tool convex and concave form roughness center plane become equal). This is intended to make the measured values become equal to *Ra* of 2D asperity by including many asperity points when *Ra* is measured on an arbitrarily chosen section in the rolling direction. The details of the calculated conditions are shown in Fig. 36 and **Table 4**.

The analysis procedure is as follows: ① press the die tool to the work and force 1/2 of the prescribed stress in the rolling direction [STEP 1]; ② stop die tool pressing and force the remaining stress in the rolling direction [STEP 2]; ③ unload die tool and stress in the rolling direction [STEP 3]; ④ after unloading, in case elongation calculated by displacement at the free end of the work (to be provided with the stress boundary condition) does not reach the prescribed values (0.6 and 1%), further adjustment to the die tool pressing is to be made in [STEP 1], and the procedure up to [STEP 3] is to be repeated until elongation after unloading of stress reaches the pre-

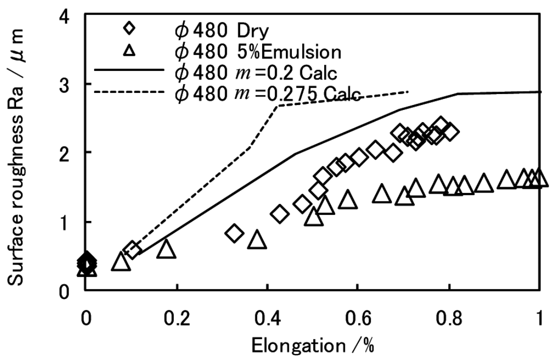

Fig. 35 Relation between surface roughness and elongation (with φ480 mm roll)

Table 4 Conditions of die press simulation

Work (rolled material)	Width 62.5 μm, Length 62.5 μm Thickness 0.1 mm (1/2 symmetry) Upper yield stress: 400 MPa Lower yield stress: 312 MPa Entry unit tension: 82 MPa
Asperity	Height (p-p) 10 μm (2D), 15 μm (3D) Pitch 62.5 μm
Pressing conditions	0.6%, 1.0% reduction Friction factor m = 0.275 (MK-model) Prescribed stress at boundary = −2 000–0 MPa

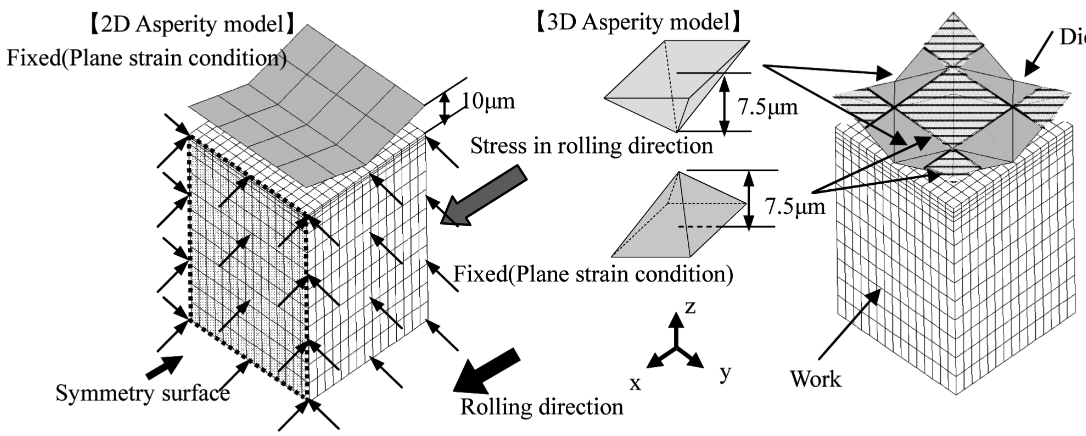

Fig. 36 2D, 3D die and work configuration and finite element mesh

scribed value. Here, the free ends of the work are constrained to always remain in a flat state in order to simulate rolling. Concerning two distinct loading steps STEP 1 and STEP 2, STEP 1 simulates the average thickness reduction from entry of the roll-bite to x = 0.7 mm in the roll-bite where the average thickness reduction stops as is observed in Fig. 29, and STEP 2 simulates increase in compressive stress in the rolling direction from x = 0.7 mm to around x = 0 mm in the roll-bite as is observed in Fig. 30.

Die-press analysis was conducted in the aforementioned procedure, and the transcribed surface roughness *Ra* of the work was sought for. Furthermore, as the transcription characteristics are considered to be compared based on an identical plasticity deformation amount, namely, elongation, the die press analysis conditions of elongation of 0.6 and 1.0% was determined taking into account the results of experiments with small and large diameter rolls, as shown in Figs. 34 and 35 and the results of their analysis. In addition, the average stress in the rolling direction to be provided as a boundary condition was set at 0−−2000 MPa based on the result of the 2D rolling analysis shown in **Fig. 37**.

(2) Examination of errors in 2D rolling roughness transcription analysis with die press analysis

In **Fig. 38**, the relationship between stress in the rolling direction and surface roughness *Ra* with respect to 2D, 3D surface asperity models, and elongation obtained with die press analysis is shown. These results reconfirmed an element of the most basic transcription principle that, in both cases of 2D and 3D asperity, the transcribed roughness *Ra* becomes larger as compressive stress in rolling direction becomes higher, regardless of the elongation as examined in the 2D analysis.

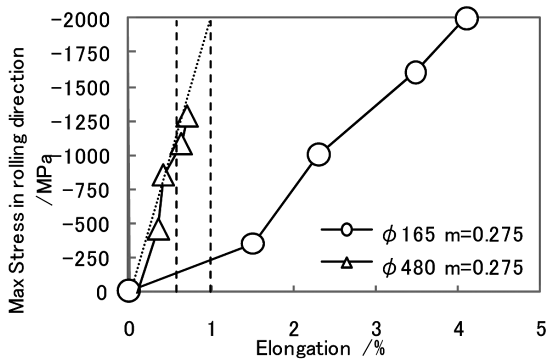

Fig. 37 Relation between stress in rolling direction and elongation

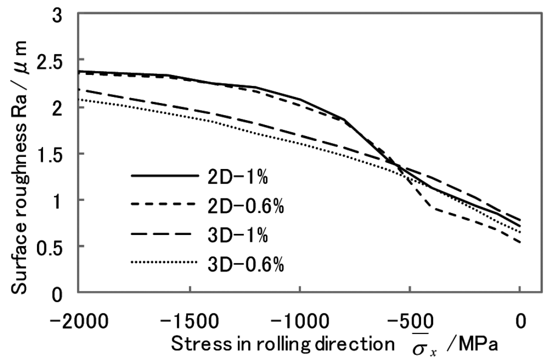

Fig. 38 Relation between surface roughness and stress in rolling direction (0.6% and 1% elongation)

Next, when the 2D and 3D transcription characteristics in Fig. 38 are compared, below the compressive stress in the rolling direction of 600 MPa, 2D and 3D asperity are almost equally transcribed, and, with higher compressive stress, 2D asperity is more easily transcribed. When this result is examined referring to the results of the 2D rolling transcription analysis shown in Figs. 34, 35, and 37, the difference in the transcription characteristics between the results of 2D rolling analysis and the experimental values becomes explainable. Specifically, it is considered that; from Fig. 37, in small diameter roll rolling, under the condition of elongation of below 2%, the compressive stress in the rolling direction becomes below 600 MPa and, in this region, transcription of 2D and 3D asperity proceeds with nearly equal efficiency. This accounts for the good agreement of 2D rolling analysis with the rolling experiment in view of roughness transcription characteristics.

On the other hand, in the case of the large diameter roll, even with an elongation of 0.6%, the compressive stress in the rolling direction grows to as high as nearly 1000 MPa, as shown in Fig. 37, and 2D asperity is transcribed more efficiently than 3D asperity in this region as shown in Fig. 38. It is understood that the roughness transcription shown in Figs. 33 and 35 is overestimated in 2D rolling analysis as compared to experiment result due to this mechanism.

Incidentally, when transcription characteristics of 3D asperity in Fig. 38 are carefully compared, it is confirmed that, as compared to the case of elongation of 0.6%, roughness *Ra* becomes larger by about 0.1–0.2 μm in case of elongation of 1.0%, and not only stress in the rolling direction (similarly stress in thickness direction, hydrostatic stress as well) but also elongation itself exerts significant influence upon transcription characteristics. This is considered to be attributed to the result of a continuous flow of material into die tool convexo-concave surface brought forth by a substantial reduction in thickness as elongation increases from 0.6 to 1%.

(3) Difference in transcription characteristics of 2D and 3D asperity and appropriateness of 2D rolling analysis.

As mentioned above, although errors caused in the 2D rolling analysis as to roughness transcription characteristics have been made explainable with the 3D die press analysis and here, the cause of difference between transcription characteristics of 2D asperity and that of 3D asperity in 3D die press analysis is examined.

Shown in **Fig. 39** is a contour figure showing the stress in plate thickness direction right before unloading in [STEP 2] in die press analysis of 2D and 3D asperity die tool. The die-press condition is; 1% of elongation and −1200 MPa of stress in rolling direction. In either die tool case, a high compressive force is exerted in the regions where the die convex is pressed in, and stress in the plate thickness

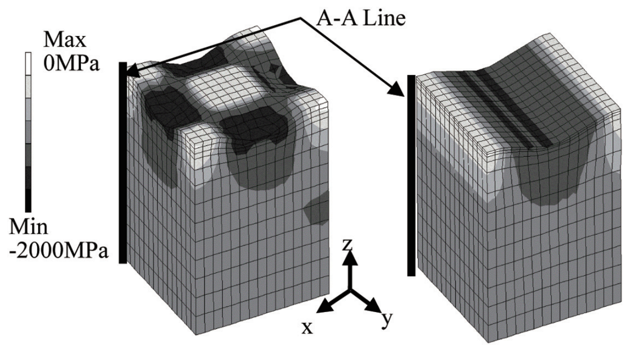

Fig. 39 Distribution of stress in thickness direction (at $\bar{\sigma}_x$ = −1 200 MPa)

direction in the die concave regions is very small. As the figure shows, the die convex is pressed to the plate material with high contact pressure and the plate deforms dependably upon die-tool configuration. However, stress in the plate thickness direction in the region of the concave of die tool is small, and the concave portion of die tool comes to be filled in with metal pushed upward in thickness direction from the center of the plate. In addition, it can be said that roughness transcription is characterized by the filling-in phenomenon of metal to the concave portion of die tool and examination should be conducted focusing on behavior of the material flow to the die tool concave portion.

Observing the state of deformation in Fig. 39 from this viewpoint, it is observed that FEM elements undergo severe shear stress in the neighborhood of the border line between the concave and convex parts of the die tool. Specifically, it is found that the material at the convex part of the die tool constrains the metal flow to the concave part of the die tool. When the 2D and 3D asperities are compared, in 3D asperity, convexo-concave configuration of the die tool exists in the width direction. As a matter of course, vertical material flow is also constrained by the adjacent portion of the metal in the width direction. Since this vertical metal flow constraint is considered to be caused mainly by shear stress acting from metal in the convex portion to that in the concave portion.

Figure 40 shows the distribution in the plate thickness direction of the absolute value of shear stress τ_{yz} acting on a symmetrical (y-z) plain averaged in the width direction. As a matter of course, in the case of 2D asperity, the shear stress is not observed at all. However, in the case of 3D asperity, the high shear stress is exerted within 1/4 thickness from the surface. As a result of this, metal filling in the concave area of the die tool is retarded by the existence of τ_{yz} in 3D asperity, and therefore the transcribed roughness is considered to become smaller than in the case of 2D asperity. When viewed at a different angle, in the 2D rolling analysis corresponding to 2D asperity, the existing constraining shear stress exerted by asperity in the width direction cannot be taken into account, and therefore the transcribed roughness is overestimated.

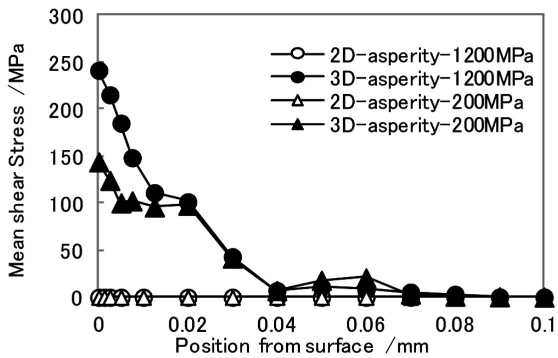

Fig. 40 Mean shear stress in symmetry surface (at $\bar{\sigma}_x$ = −1 200 MPa)

Incidentally, in Fig. 38, in the case of 2D asperity, the transcribed roughness decreases in a stepwise manner as the compressive stress in the rolling direction becomes smaller, and consequently, coming to the transcribed roughness equivalent to the one in case of 3D asperity. It is considered that, under the rolling condition with a small diameter roll, where compressive stress in the rolling direction is small, these findings suggest that the result of the 2D rolling analysis in terms of the transcribed roughness approximately agrees with the result of the experiment which is shown in Fig. 32.

To examine the cause of this, the equivalent plastic strain distribution (in 0–0.1 range) before unloading in [STEP 2] in cases of 200 and 1200 MPa of compressive stress in the rolling direction in die press analysis with 2D and 3D asperity (elongation 0.6%) is shown in **Fig. 41**. In the Figure, in the case of 3D asperity, although the difference in magnitude of the equivalent plastic strain due to the difference in compressive stress in the rolling direction is apparent, plastic strain is observed in the entire work, and no change in strain mode is observed.

On the other hand, it is observed that in the case of 2D asperity, with a compressive stress in the rolling direction of 1200 MPa, significant plastic strain is observed in the entire area of contact with the die tool. However, under the condition of compressive stress in the rolling direction of 200 MPa, portion of no plastic strain in the material corresponding to the die tool concave area is observed. As mentioned above in this section, transcription phenomenon is characterized by the fill-in of material in the die tool concave. Therefore, if the material in this portion is not plastic-deformed, transcription of die tool asperity is impeded, and, with this, surface roughness after pressing-in of die asperity in Fig. 38 is considered to decrease in a stepwise manner as compressive stress in the rolling direction becomes smaller.

6.2 Proposal of roughness prediction method by means of 2D rolling analysis and 3D die press analysis

Through study and examination by means of the above experimental and numerical analysis, it was clarified that the roughness transcription phenomenon in skin pass rolling depends on the rolling pressure along the roll bite, the thickness-direction average value of

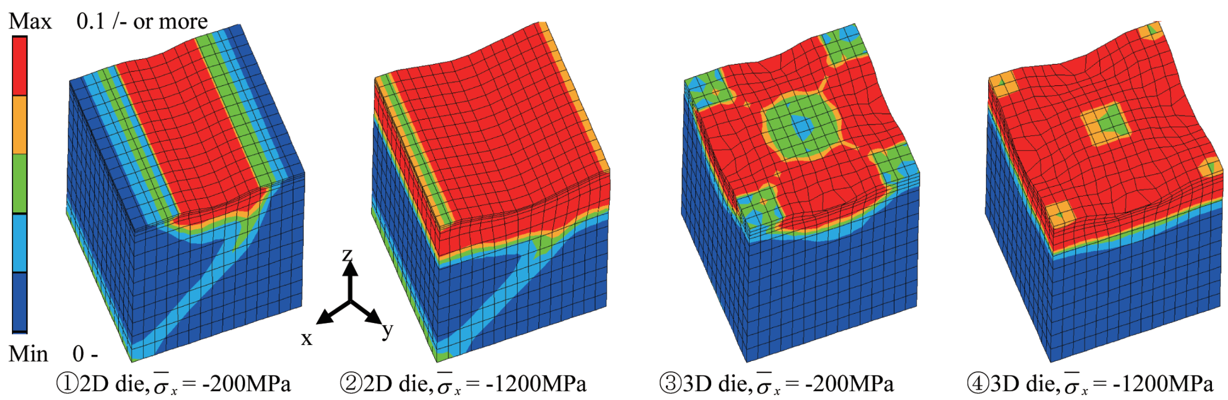

Fig. 41 Distribution of equivalent plastic strain (at stress in rolling direction −200 MPa or −1 200 MPa, elongation 0.6%)

stress in the rolling direction which represents hydrostatic stress, and the elongation. And roughness transcription obtained with 2D rolling analysis contains two essential error factors. These factors are: ① transcription is overestimated as constrain by shear stress exerted by an adjacent material in the widthwise direction cannot be taken into account; and ②, in case the compressive stress in the rolling direction is small, an unrealistic, non-plastic deformation region is formed in the material in roll concave portion and thereby, transcription is underestimated.

In the rolling conditions taken up in this paper, although the transcription results which almost agree with the experimental values are obtained with 2D rolling analysis under the condition of small compressive stress in the rolling direction, this result is inappropriate to be rationalized in general since there are two different error causes and it should be considered that they happened to almost cancel with each other in the the relevant rolling conditions. Hence, as for the roughness transcription phenomenon, 2D rolling analysis needs to be considered as containing errors. It is considered that these problems could be solved by applying 3D rolling analysis wherein roll deformation and roll surface roughness are appropriately taken into account; however the analysis cannot be used as a practical calculation method because amount of computation time and cost required would not be acceptable in view of current computer capacity. Hence,the authors propose a practical roughness transcription predicting method developed by combining the 2D rolling analysis and the 3D die press analysis used in this report.

As mentioned previously, with the 2D rolling analysis linked to roll deformation proposed in this research, good agreement with experimental data even in dull work roll rolling is obtained in terms of rolling force and elongation. Agreements in rolling force and elongation are considered to confirm that the calculation as to the macroscopic state of stress in the roll bite which determines rolling force is valid. In brief, the method is as follows. Based on a given rolling condition (including elongation), conduct 2D rolling analysis and calculate the rolling-direction average stress value in the plate thickness direction, and then extract the maximum value from the roll bite. After this, provide the stress in the rolling direction and elongation, and conduct 3D die press analysis under the 3D asperity condition as shown in Fig. 36 and Table 4. Finally, predict the roughness after rolling.

In **Fig. 42**, roughness predicted with the aforementioned method under the condition of elongation of 0.6% for a 480 mm diameter roll, and the condition where elongation is 1% for a 165 mm diameter roll are marked as ◆ and ▲, respectively. The results shown in Figs. 34 and 35 show good agreement with the experimental results.

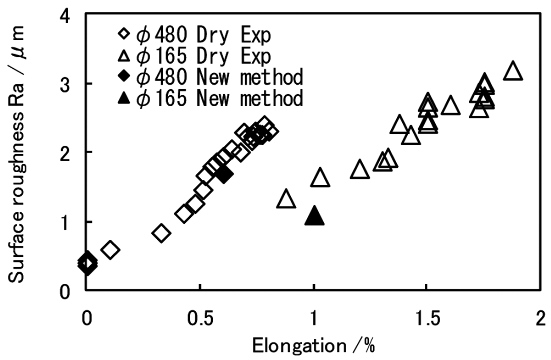

Fig. 42 Prediction of surface roughness by proposed method

Further, validation of this method under a wider range of rolling conditions remains to be an issue for future research.

7. Conclusion

In order to clarify the skin pass rolling characteristics of ultrathin steel plate, an experiment using a laboratory rolling mill with a large diameter roll and numerical analysis based on elastoplasticity finite element method under the experimental conditions were conducted, and the following results are obtained.

1) In the dull work roll rolling, elongation gradually increases as rolling force increases. However, when compared with the case of bright work roll rolling, elongation is large in the low force region before jumping and becomes remarkably small in the high force region after jumping.
2) By using a 2D rolling numerical analysis method which takes into account not only elastoplasticity deformation of the rolled plate, but also the elastic deformation of the roll appropriately, and by modelling roll surface asperity appropriately with a triangular shape, dull work roll rolling characteristics obtained by the experiment could be accurately reproduced.
3) It was clarified that the characteristics of the relationship between rolling force and elongation is explainable with two factors: first, the effect of local plastic deformation caused by roll surface asperity penetrating through plates in thickness direction and second, the geometrical friction effect caused by roll surface asperity.
4) It was clarified that the effect of geometrical friction on the roll surface asperity is governed by the asperity slope angle.
5) It was clarified that roughness transcription phenomenon depends on the rolling pressure in roll bite and thickness-direction average value of stress in the rolling direction which represents hydrostatic pressure and elongation, and that, as to roughness transcription, 2D rolling analysis includes two essential error factors; an error caused by neglecting the shear stress in width direction, and another error of developing unrealistic deformation mode change.
6) To solve the problem of transcription prediction with 2D rolling analysis, simplified roughness prediction methods developed by combining 2D rolling analysis with 3D die press analysis was proposed.

References

1) Shiraishi, T., Akashi, T., Takahama, Y., Ogawa, S.: Journal of the Japan Society for Technology of Plasticity. 51 (597), 969–973 (2010)
2) Matsumoto, H.: Final Report of Study Group for Skin Pass Rolling Microscopic Deformation Analysis. The Iron and Steel Institute of Japan, 2007, p.25–34
3) Yarita, M., Ito, M.: Tetsu-to-Hagané. 94 (10), 405–414 (2008)
4) Yoshida, F., Kaneda, Y., Yamamoto, S.: Int. J. Plasticity. 24, 1792–1818 (2008)
5) Yarita, M., Ito, M.: Tetsu-to-Hagané. 94 (10), 391–398 (2008)
6) Ike, H.: Final Report of Study Group for Skin Pass Rolling Microscopic Deformation Analysis. The Iron and Steel Institute of Japan, 2007, p.99–110
7) Yukawa, N., Akiyama, T., Yoshida, Y., Ishikawa, T.: Tetsu-to-Hagané. 94 (10), 399–404 (2008)
8) Akashi, T., Shiraishi, T., Ogawa, S., Matsuse, Y.: CAMP-ISIJ. 24, 909 (2011)
9) Kijima, H.: J. Mat. Proc. Technol. 214, 1111–1119 (2014)
10) Akashi, T., Shiraishi, T., Ogawa, S., Matsuse, Y.: Journal of the Japan Society for Technology of Plasticity. 54 (630), 606–611 (2013)
11) Akashi, T., Shiraishi, T., Ogawa, S., Matsuse, Y.: Journal of the Japan Society for Technology of Plasticity. 55 (639), 324–330 (2014)
12) Akashi, T., Shiraishi, T., Ogawa, S., Matsuse, Y., Morihara, H.: Journal

of the Japan Society for Technology of Plasticity. 56 (648), 53–59 (2015)
13) Nagase, N., Shido, S., Yarita, M.: Tetsu-to-Hagané. 94 (10), 429–437 (2008)

Tooru AKASHI
Chief Researcher, Dr.Eng.
Integrated Process Research Lab.
Process Research Laboratories
20-1 Shintomi, Futtsu City, Chiba Pref. 293-8511

Toshiyuki SHIRAISHI
Senior Researcher, Dr.Eng.
Steel Rolling Research Lab.
Process Research Laboratories

Shigeru OGAWA
Executive Advisor, Dr.Eng.

Yoshihito MATSUSE
Chief Manager
Simulation Engineering Solution Dept.
NS Plant Designing Corporation

Hideyuki MORIHARA
Manager
CAE Section
SANKI Engineering Corporation